

# Development and Evaluation of Proportional-Derivative, Proportional-Derivative with Friction Compensation, Inverse-Dynamics, and Sliding-Mode Control Strategies for Trajectory-Tracking in Robotic Manipulators <sup>†</sup>

David Robles <sup>1</sup>, Ney Medrano <sup>1</sup>, Yuliana Chicay <sup>1</sup>, Marjorie Pilatasig <sup>1</sup>, Gabriela M. Andaluz <sup>1,2</sup> and Paulo Leica <sup>1,\*</sup>

<sup>1</sup> Departamento de Automatización y Control Industrial, Facultad de Ingeniería Eléctrica y Electrónica, Escuela Politécnica Nacional, Quito 170525, Ecuador; ney.medrano@epn.edu.ec (N.M.); gabriela.andaluz@epn.edu.ec (G.M.A.)

<sup>2</sup> Department of Electronic Engineering and Communications, Universidad de Zaragoza, 44003 Zaragoza, Spain  
\* Correspondence: paulo.leica@epn.edu.ec

<sup>†</sup> Presented at the XXXII Conference on Electrical and Electronic Engineering, Quito, Ecuador, 12–15 November 2024.

**Abstract:** In this paper, four control strategies are developed and evaluated for the trajectory-tracking of a two-degree-of-freedom SCARA-type robotic manipulator: (i) a proportional-derivative controller (PD), (ii) a proportional-derivative controller with friction compensation (PD + G), (iii) an inverse-dynamics controller and (iv) a sliding-mode controller with a dynamic model (SMCD). These controllers are implemented in a dynamic model of a manipulator robot, and their performance is assessed based on trajectory-tracking accuracy and robustness against disturbances. Robustness tests are conducted by varying the parameters of the dynamic model of the robot. The performance of each controller is analyzed using the Integral Squared Error (ISE) and the Integral of Time-weighted Squared Error (ITSE) indexes to compare their effectiveness. This study offers a comprehensive evaluation of each control strategy, demonstrating that the SMCD achieves the optimal balance between accuracy and disturbance robustness.

**Keywords:** inverse dynamics; manipulator; trajectory-tracking; PD controller; robustness; SMC



**Citation:** Robles, D.; Medrano, N.; Chicay, Y.; Pilatasig, M.; Andaluz, G.M.; Leica, P. Development and Evaluation of Proportional-Derivative, Proportional-Derivative with Friction Compensation, Inverse-Dynamics, and Sliding-Mode Control Strategies for Trajectory-Tracking in Robotic Manipulators. *Eng. Proc.* **2024**, *77*, 18. <https://doi.org/10.3390/engproc2024077018>

Academic Editor: Pablo Proaño

Published: 18 November 2024



**Copyright:** © 2024 by the authors. Licensee MDPI, Basel, Switzerland. This article is an open access article distributed under the terms and conditions of the Creative Commons Attribution (CC BY) license (<https://creativecommons.org/licenses/by/4.0/>).

## 1. Introduction

Robotic manipulators are fundamental components of industrial automation and play a critical role in tasks that require precision, repeatability, and flexibility. However, the precise control of these systems remains a complex challenge and of interest to researchers, especially when faced with model uncertainties, external disturbances, and dynamic motions [1]. Several control strategies have been developed to control a robotic manipulator [2,3].

There are controllers as in [4], which employ improved classical techniques such as adaptive PID that do not depend on the model and are robust to load variations. However, nonlinear controllers, such as sliding-mode controllers (SMCs), efficiently improve the tracking of the robotic manipulator [5]. The proposal of [6] focuses on the improvement of chattering by using three SMCs with the sign function, saturation, and hyperbolic tangent function—the SMC with saturation had the best results. In [7], an SMC + PD is implemented with an algorithm that does not require knowledge of the robot model, so the SMC is induced to consider the robot dynamics as an uncertainty and avoid using the model. It is worth noting the superiority in the efficiency of SMCs over classical controllers such as PDs, whose steady-state error is notoriously higher compared to an SMC-type controller [8]. SMCs have also been combined with fuzzy techniques to improve controller performance [9]. One of the challenges of SMCs is

implementing techniques to mitigate the chattering effect through controller stability analysis using Lyapunov theory [10] and other SMC controls with backstepping [11]. In the work presented in [12], it is observed that the determination of an unsteady sliding surface improves the implemented control law for the sliding-mode controller; however, the control is applied to the robot joints and not to the trajectory generation. In [13–16], emphasis is placed on the implementation of a robust controller based on the sliding mode for the trajectory-tracking of a robotic manipulator; however, these works do not present a robustness analysis of the variation present in the model.

The main contributions of this work are that the controller works on the end-effector error and not on the joints, allowing us to take advantage of the redundancy of the manipulator. Another contribution corresponds to the design of an SMC that is based on the robot model, thus obtaining a controller robust to model variations, unlike other works where the perturbations are considered in the references or at the output and not with regard to the model. Also, in the design, the discontinuous component has been considered as a variant of the sigmoid to improve the chattering of the system. Another proposal of this work is the comparison through the development and evaluation of four control strategies for the trajectory-tracking of a SCARA-type robotic manipulator: (i) a proportional-derivative (PD) controller; (ii) a PD controller with friction compensation (PD + G); (iii) an inverse-dynamics controller; and (iv) a sliding-mode controller with a dynamic model (SMCD). This includes the formulation of the cinematic and dynamic model of the manipulator robot and the design of the SMCD, which includes an optimized sliding surface and a control law based on Lyapunov's theory, ensuring superior robustness to system perturbations. The validation of the proposed approach is performed by a simulation of the robotic manipulator, including trajectory algorithms, and the implementation of several test scenarios that allow for a comprehensive evaluation of the position error. The use of the Integral Squared Error (ISE) and Integral of Time-weighted Squared Error (ITSE) indexes allows for measuring the performance of the controllers, providing a quantitative comparison.

This paper is organized as follows: Section 2 presents the modeling of the SCARA-type manipulator robot; Section 3 describes the four implemented controllers; Section 4 outlines the simulation level tests of the controllers and the results of the system under perturbations; and finally, Section 5 provides the conclusions obtained from the results of the development and evaluation of the controllers.

## 2. Modeling

The manipulator robot used in this work is of an industrial type and corresponds to a SCARA-type structure (model BOSCH SR-800 of German origin), which has two degrees of freedom. The implementation of the four control strategies requires knowledge of its kinematic and dynamic models, which are described below.

### 2.1. Kinematic Model of the Manipulator Robot

The kinematic model of the two-degree-of-freedom SCARA manipulator shown in Figure 1 relates the position of the operating end in the  $(x, y)$  plane to the variables of the two joints  $q_1, q_2$ .  $(x, y)$  is the referential plane of the end-effector position, and  $q_1$ , and  $q_2$ , are the angular positions of joint 1 and 2, respectively. The robot parameters are the length of the first link,  $l_1 = 0.445$  m, and the length of the second link,  $l_2 = 0.355$  m, [17]. The kinematic model of the robot is defined by

$$x = l_1 \cos(q_1) + l_2 \cos(q_1 + q_2); \quad y = l_1 \sin(q_1) + l_2 \sin(q_1 + q_2) \quad (1)$$

The inverse kinematics of the robot can be obtained by means of geometric analysis:

$$q_1 = \tan^{-1}\left(\frac{y}{x}\right) - \tan^{-1}\left(\frac{l_2 - \sin(q_2)}{l_1 + l_2 \cos(q_2)}\right) \quad (2)$$

$$q_2 = \cos^{-1} \left( \frac{x^2 + y^2 - l_1^2 - l_2^2}{2l_1l_2} \right) \quad (3)$$

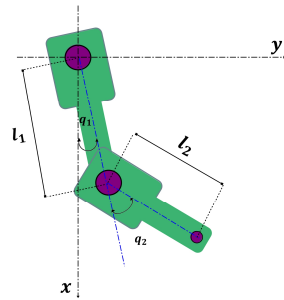


Figure 1. SCARA robotic manipulator.

From the derivation of (1), the kinematic model can be represented as

$$\begin{bmatrix} \dot{\tilde{x}} \\ \dot{\tilde{y}} \end{bmatrix}^T = J(q) \begin{bmatrix} \dot{\tilde{q}}_1 \\ \dot{\tilde{q}}_2 \end{bmatrix}^T \quad (4)$$

$\begin{bmatrix} \dot{\tilde{x}} \\ \dot{\tilde{y}} \end{bmatrix}^T$  is the derivative of the error in  $x$  and  $y$ , respectively;  $\begin{bmatrix} \dot{\tilde{q}}_1 \\ \dot{\tilde{q}}_2 \end{bmatrix}^T$  is the derivative of the angular error of joint 1 and 2; and  $J(q)$  is the Jacobian matrix, which is given by

$$J(q) = \begin{bmatrix} -(l_1 \sin(q_1) + l_2 \sin(q_1 + q_2)) & -l_2 \sin(q_1 + q_2) \\ (l_1 \cos(q_1) + l_2 \cos(q_1 + q_2)) & l_2 \cos(q_1 + q_2) \end{bmatrix} \quad (5)$$

### 2.2. Robot Dynamic Model

The dynamic model for the SCARA robotic arm with two degrees of freedom is defined as

$$\ddot{q} = M^{-1}(q) (\tau - C(q, \dot{q})\dot{q} - f(\dot{q})) \quad (6)$$

$\tau$  is the vector of torques of joints 1 and 2, respectively;  $M(q)$  is the inertia matrix of the manipulator robot;  $C(q, \dot{q})$  is the matrix representing the centrifugal and Coriolis forces; and  $f(\dot{q})$  is the vector representing the effects of viscous friction. The dynamic parameters of the Bosh SR-800 manipulator robot are obtained from [17].

$$M(q) = \begin{bmatrix} 1.7277 + 0.1908 \cos(q_2) & 0.0918 + 0.0954 \cos(q_2) \\ 0.0918 + 0.0954 \cos(q_2) & 0.9184 \end{bmatrix} \quad (7)$$

$$C(q, \dot{q}) = \begin{bmatrix} 31.8192 - 0.0954 \sin(q_2) \dot{q}_2 & -0.0954 \sin(q_2) (\dot{q}_1 + \dot{q}_2) \\ 0.3418 \sin(q_2) \dot{q}_1 & 12.578 \end{bmatrix} \quad (8)$$

$$f(\dot{q}) = \begin{bmatrix} 1.0256 \operatorname{sig}(\dot{q}_1) \\ 1.7842 \operatorname{sig}(\dot{q}_2) \end{bmatrix} \quad (9)$$

## 3. Controllers

Four control strategies for trajectory-tracking the SCARA-type manipulator robot are presented: (i) a proportional-derivative (PD) controller, (ii) a PD controller with friction compensation (PD + G), (iii) an inverse-dynamics controller, and (iv) a sliding-mode controller with a dynamic model (SMCD).

### 3.1. Dynamic Sliding Mode Controller (SMCD)

The controller in sliding mode with a dynamic model allows us to improve the performance of the system. Since it considers the dynamics of the manipulator, it will allow us to reduce the position error in the steady state, which means  $\tilde{p} \rightarrow 0$  as time tends to

infinity  $\lim_{t \rightarrow \infty} \tilde{p} = 0 \in R^n$ . The sliding-mode control structure with a dynamic model (SMCD) is defined as the following:

$$\tau_{SMCD} = \tau_{cD} + \tau_{dD} \quad (10)$$

where  $\tau_{SMCD}$  describes the SMCD control action;  $\tau_{cD}$  represents the continuous part; and  $\tau_{dD}$  represents the discontinuous part of the control action. Figure 2 shows the SMCD controller scheme, where  $\varepsilon_d$  represents the robot's desired trajectory and  $\varepsilon$  represents the trajectory described by the robot.

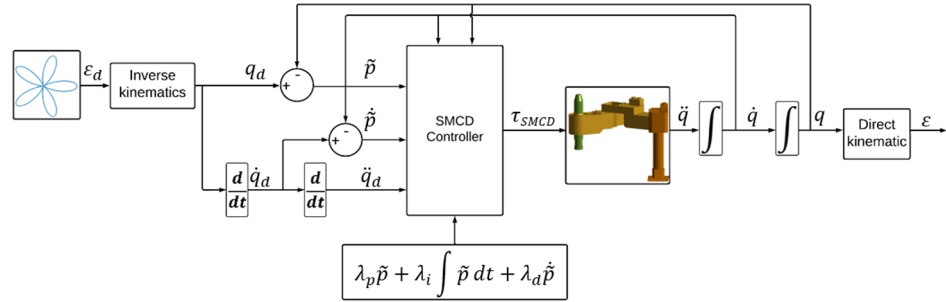


Figure 2. SMCD control scheme.

The sliding surface is defined by

$$s = \lambda_p \tilde{p} + \lambda_i \int \tilde{p} dt + \lambda_d \dot{\tilde{p}} \quad (11)$$

where  $\tilde{p} = [q_d - q]$  is the end-effector position error;  $q_d$  represents the desired end-effector positions;  $q$  is the current position of the robot end effector;  $\lambda_p$ ,  $\lambda_i$ , and  $\lambda_d$  are the coefficients of the proportional, integral, and derivative parts of the sliding surface, respectively.  $\dot{\tilde{p}} = [\dot{q}_d - \dot{q}]$  is the error of the end-effector velocity;  $\dot{q}_d$  is the desired velocity of the end effector;  $\ddot{\tilde{p}} = [\ddot{q}_d - \ddot{q}]$  is the acceleration error;  $\ddot{q}_d$  is the desired end-effector acceleration; and  $\ddot{q}$  is the acceleration of the robot end-effector. Deriving (11) and substituting  $\ddot{\tilde{p}} = \ddot{q}_d - \ddot{q}$ , we obtain (12):

$$\dot{s} = \lambda_p \dot{\tilde{p}} + \lambda_i \tilde{p} + \lambda_d (\ddot{q}_d - \ddot{q}) \quad (12)$$

Substituting (6) in (12), we obtain the following expression:

$$\dot{s} = \lambda_p \dot{\tilde{p}} + \lambda_i \tilde{p} + \lambda_d (\ddot{q}_d - M^{-1}(q) (\tau - C(q, \dot{q})\dot{q} - f(\ddot{q}))) \quad (13)$$

To determine  $\tau_{cD}$ , we assume  $\tau_{dD} = 0$  and set  $\dot{s} = 0$ , obtaining (14):

$$\tau_{cD} = M(q) \left[ \frac{\lambda_p \dot{\tilde{p}}}{\lambda_d} + \frac{\lambda_i \tilde{p}}{\lambda_d} + \ddot{q}_d \right] + C(q, \dot{q})\dot{q} + f(\ddot{q}) \quad (14)$$

For  $\tau_{dD}$ , the Lyapunov candidate function is defined as  $V = \frac{1}{2} s^T s$ . Deriving  $V$  with respect to time,  $\dot{V} = s^T \dot{s}$  is obtained. Substituting (12) and in a closed loop,  $\tau = \tau_{SMCD} = \tau_{cD} + \tau_{dD}$ , and replacing (14), we obtain the following:

$$\dot{V} = s^T (-M^{-1} \lambda_d \tau_{dD}) \quad (15)$$

To ensure that  $\dot{V} < 0$ ,  $\tau_{dD}$  is defined as

$$\tau_{dD} = \lambda_d^{-1} M \delta \frac{s}{|s| + \beta} \quad (16)$$

where  $\delta$  and  $\beta$  represent a positive scalar;  $sign(s)$  is a sign function. We substitute (16) in (15).

$$\dot{V} = -s^T \delta \frac{s}{|s| + \beta} \quad (17)$$

This guarantees that  $\dot{V} < 0$ ; therefore,  $s \rightarrow 0$  as  $t \rightarrow \infty$ . Deriving (11) and setting it equal to zero, we obtain the following:

$$0 = \lambda_d \ddot{\tilde{p}} + \lambda_p \dot{\tilde{p}} + \lambda_i \tilde{p} \quad (18)$$

The roots of the second-order system can be defined as  $r = \frac{-\lambda_p - \sqrt{\lambda_p^2 - 4\lambda_d\lambda_i}}{2\lambda_d}$ . In this second-order system, to have different real roots, it must be satisfied that  $\lambda_p^2 > 4\lambda_d\lambda_i$ ; then,  $\tilde{p} \rightarrow 0$  with  $t \rightarrow \infty$ .

### 3.2. Inverse-Dynamics Controller

The control law used to implement the model is taken from [18], and is defined as follows:

$$\tau = M(q) \left( \ddot{q}_d + K_v \dot{\tilde{q}} + K_p \tilde{q} \right) + C(q, \dot{q}) \dot{q} + f(\dot{q}) \quad (19)$$

where  $\dot{\tilde{q}} = [\dot{q}_d - \dot{q}]$  is the end-effector velocity error;  $\dot{q}_d$  is the desired end-effector speed;  $\dot{q}$  is the manipulator robot end-effector speed;  $\tilde{q} = [q_d - q]$  is the end-effector position error; and  $K_v$  and  $K_p$  represent the velocity and position gain matrices, respectively.

### 3.3. Controller PD + G

For the PD + G controller, the following control law given in [19] is used, described by

$$\tau = K_v \dot{\tilde{q}} + K_p \tilde{q} + f(\dot{q}) \quad (20)$$

### 3.4. Controller PD

For the PD controller, we use the control law given in [19], which is defined as follows:

$$\tau = K_v \dot{\tilde{q}} + K_p \tilde{q} \quad (21)$$

## 4. Results

In order to compare the four controllers, the tests of all the controllers consist of the manipulator robot tracking a trajectory of a five-petal flower. The parameters of the desired trajectory are as follows:  $r = 0.1 + 0.1 \cos(0.25t)$ ;  $x_d = r \cos(0.05t) + 0.4$ ; and  $y_d = r \sin(0.05t) + 0.4$ , where  $\varepsilon_d = [x_d \ y_d]$  and  $\varepsilon = [x \ y]$ . The parameters of the proportional and derivative actions of the PD controller are  $K_p = \begin{bmatrix} 40 & 0 \\ 0 & 40 \end{bmatrix}$  and  $K_v = \begin{bmatrix} 10 & 0 \\ 0 & 10 \end{bmatrix}$ , and those of the PD + G controller are  $K_p = \begin{bmatrix} 40 & 0 \\ 0 & 20 \end{bmatrix}$  and  $K_v = \begin{bmatrix} 20 & 0 \\ 0 & 14 \end{bmatrix}$ . The parameters of the proposed SMCD are  $\lambda_p = 0.1$ ,  $\lambda_i = 70$ ,  $\lambda_d = 0.5$ ,  $\beta = 0.6$ ; and  $\delta = 1.2$ . To analyze the behavior of the controllers, it is proposed to develop two experiments. A time of 130 s is considered the simulation duration of Experiment 1, and 260 s is the simulation duration of Experiment 2. In Experiment 1, the desired trajectory is implemented without any disturbance. In Experiment 2, the desired trajectory is considered with disturbance at time  $t = 130$  s. For both experiments, two error-tracking indices are evaluated: ISE and ITSE. The simulation platform used in this work is Matlab version R2022B.

### 4.1. Experiment 1

Using the dynamic model from (6), each of the four controllers was implemented. Figure 3 shows the trajectory-tracking performance achieved by each controller. The results show that the trajectory-tracking signals described by the PD controller exhibit the highest error, while the SMCD achieves the most precise trajectory-tracking. Figure 4 shows the position errors for each controller. From the results obtained, the SMCD performs better than the others, since it has a lower amplitude and the error is visually negligible compared to the PD, PD + G, and inverse-dynamics controllers.

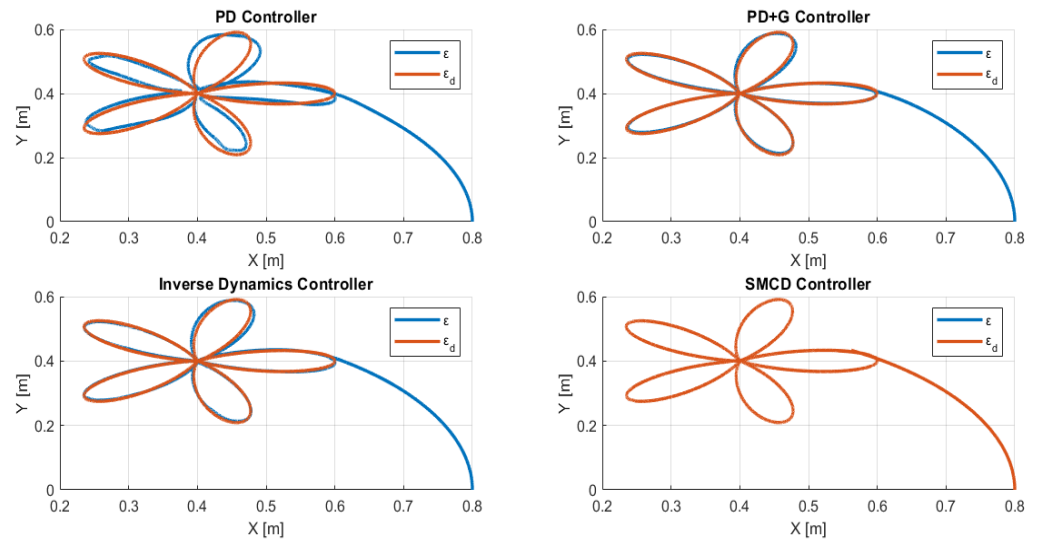


**Figure 3.** Trajectories achieved by each controller without disturbance conditions.

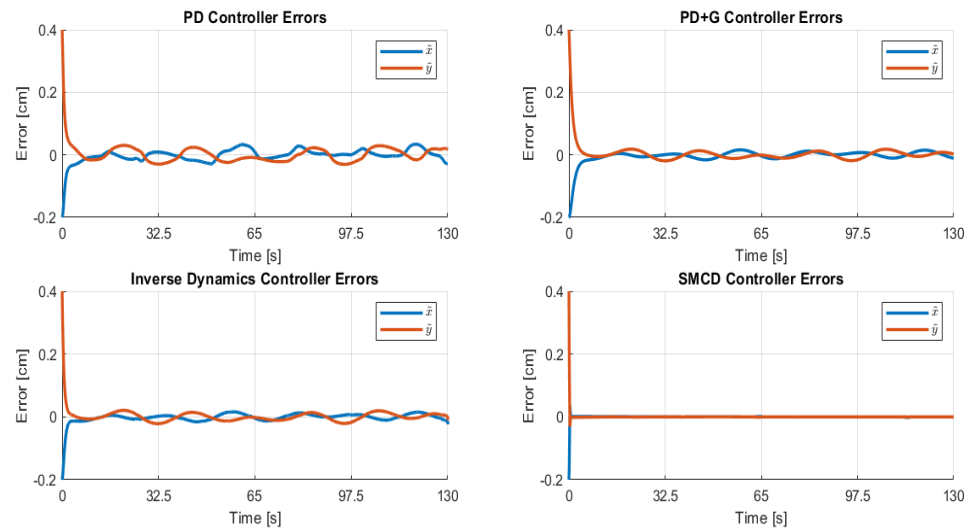


**Figure 4.** Position errors were obtained for each controller without disturbance.

Table 1 shows the error-based performance indices (ISE and ITSE) for the four controllers. From the results shown, it is observed that the values obtained for the SMCD have the lowest indices, so it is verified that it is the best controller in terms of trajectory-tracking without disturbance. On the other hand, the PD controller is the least accurate due to its high error rates.

**Table 1.** Performance index based on trajectory-tracking error with each type of controller.

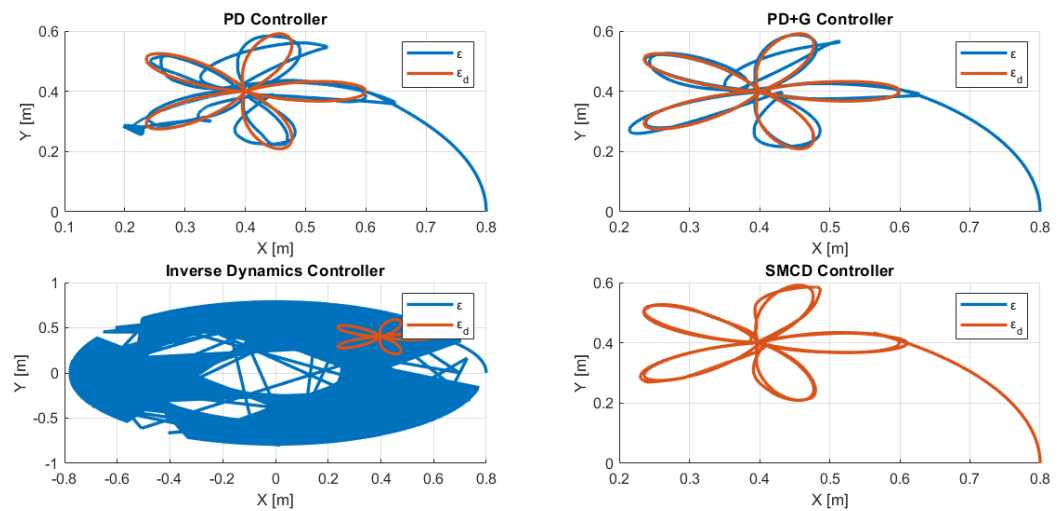
Error-Based Performance Index	PD		PD + G		Inverse Dynamics		SMCD	
	X-axis	Y-axis	X-axis	Y-axis	X-axis	Y-axis	X-axis	Y-axis
ISE	0.05944	0.1115	0.0584	0.1068	0.0334	0.0624	0.00503	0.0125
ITSE	1.913	2.99	0.6313	0.8451	0.5995	0.9947	0.00150	0.00083

4.2. Experiment 2

For the robustness analysis, a perturbation is incorporated into the matrix  $M(q)$  obtained in (7); this disturbance factor is referred to as  $F_p$ . For the analysis with perturbation, each controller has a different perturbation factor,  $F_p$ . However, the disturbance in all controllers is considered to occur at the time instant of 130 s.

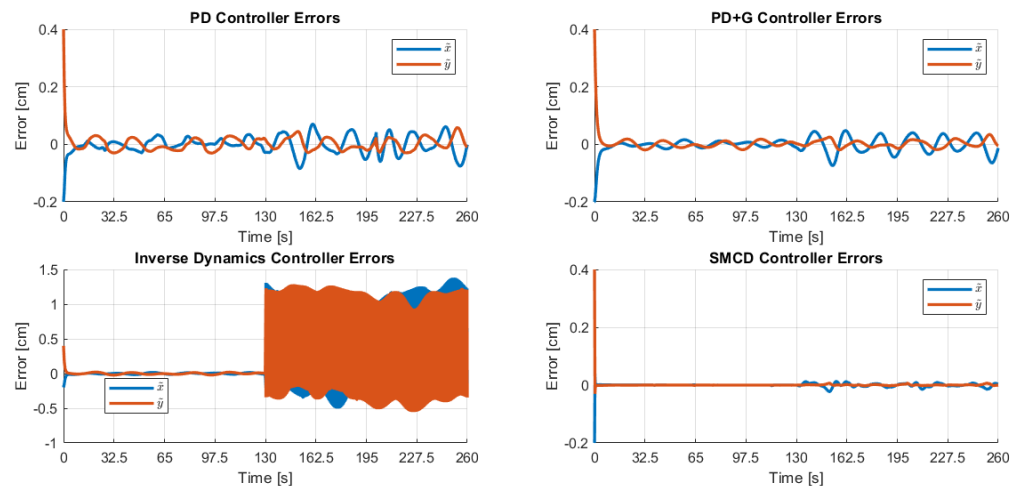
$$M(q) = \begin{bmatrix} 1.7277 + 0.1908\cos(q_2) & 0.0918F_p + 0.0954\cos(q_2) \\ 0.0918F_p + 0.0954\cos(q_2) & 0.9184F_p \end{bmatrix} \quad (22)$$

Figure 5 displays the trajectories obtained by incorporating the maximum allowed disturbance magnitude for each controller without compromising their execution capability. The results indicate that the SMCD exhibits superior performance in trajectory-tracking under disturbance conditions. In contrast, the other controllers—PD, PD + G, and inverse dynamics—experience significant destabilization due to the disturbance, and they deviate notably from the desired trajectory.



**Figure 5.** Trajectories achieved by each controller under disturbance conditions.

Finally, Figure 6 presents the position error values obtained by introducing the disturbance into the system. An analysis of the different results reveals that the error magnitude increases at the moment of disturbance occurs; despite the control actions of the different controllers, they fail to minimize the position error. The ability of each controller to handle the maximum disturbance without losing control and becoming unstable was evaluated. As a result, we found that the PD controller can tolerate a disturbance of  $F_p = 110$ , the PD + G controller can tolerate  $F_p = 90$ ; the inverse-dynamics controller can tolerate  $F_p = 82$ , and the SMCD can tolerate  $F_p = 163$ , making the SMCD the most robust against disturbances.



**Figure 6.** Position errors were obtained for each controller with disturbance at  $t = 130$  s.

## 5. Conclusions

The SMCD demonstrated significant superiority in trajectory-tracking the robotic manipulator, outperforming the other evaluated controllers both under normal conditions and with disturbances. This controller exhibited the lowest error indices (ISE and ITSE) and maintained good accuracy, even in the presence of external disturbances, highlighting its robustness and effectiveness for applications in dynamic environments. In contrast, the inverse-dynamics controller showed good performance under normal conditions but displayed notable limitations in handling disturbances, suggesting that it may not be suitable for robotic systems that require high precision and operate in dynamic environments. Meanwhile, the PD and PD + G controllers experienced considerable increases in position error when faced with disturbances, resulting in inferior performance compared to the SMCD. These results underscore the importance of considering robustness and disturbance-recovery capability in the controller design of robotic systems intended to operate in non-ideal environments.

**Author Contributions:** This work presents the development and evaluation of PD, PD + G, inverse-dynamics, and sliding-mode control strategies for trajectory-tracking in a robotic manipulator. For the development, the contribution was as follows: Conceptualization: G.M.A. and P.L.; Investigation and Methodology: G.M.A. and P.L.; Software and Validation: D.R., N.M., Y.C. and M.P.; Writing—original draft preparation: D.R., N.M., Y.C. and M.P.; Writing—review and editing: G.M.A. and P.L.; Supervision: P.L. All authors have read and agreed to the published version of the manuscript.

**Funding:** This research received no external funding.

**Institutional Review Board Statement:** Not applicable.

**Informed Consent Statement:** Not applicable.

**Data Availability Statement:** Data are contained within the article.

**Acknowledgments:** The authors would like to thank the GIECAR group and ARCI for the technical support for the work carried out. Also, the ESPE-LA and Escuela Politécnica Nacional that through the PIEX-DACI-ESPE-24 project, Autonomous control of Aerial Manipulator Robots, and PIS-23-09 have provided research hours for the development of the project.

**Conflicts of Interest:** The authors declare no conflicts of interest.

## References

1. Nuhel, A.K.; Sazid, M.M.; Bhuiyan, N.M.; Arif, A.I. Designing and Performance-Analysis of a 3 DOF Robotic Manipulator Arm and its Higher Order Integration of 7 DOF Robotic Arm. In Proceedings of the 2022 4th International Conference on Sustainable Technologies for Industry 4.0 (STI), Dhaka, Bangladesh, 17–18 December 2024. [\[CrossRef\]](#)
2. Khan, G.D. Adaptive Neural Network Control Framework for Industrial Robot Manipulators. *IEEE Access* **2024**, *12*, 63477–63483. [\[CrossRef\]](#)
3. Dai, L.; Yu, Y.; Zhai, D.-H.; Huang, T.; Xia, Y. Robust Model Predictive Tracking Control for Robot Manipulators with Disturbances. *IEEE Trans. Ind. Electron.* **2021**, *68*, 4288–4297. [\[CrossRef\]](#)
4. Lee, J.; Chang, P.H.; Yu, B.; Jin, M. An Adaptive PID Control for Robot Manipulators Under Substantial Payload Variations. *IEEE Access* **2020**, *8*, 162261–162270. [\[CrossRef\]](#)
5. Truong, T.N.; Vo, A.T.; Kang, H.-J. A Backstepping Global Fast Terminal Sliding Mode Control for Trajectory Tracking Control of Industrial Robotic Manipulators. *IEEE Access* **2021**, *9*, 31921–31931. [\[CrossRef\]](#)
6. Animesh, A.; Ohri, J. Trajectory Tracking in a 3-DOF Robotic Manipulator using Sliding Mode Controller. In Proceedings of the 2020 First IEEE International Conference on Measurement, Instrumentation, Control and Automation (ICMICA), Kurukshetra, India, 24–26 June 2020. [\[CrossRef\]](#)
7. Ouyang, P.; Acob, J.; Pano, V. PD with sliding mode control for trajectory tracking of robotic system. *Robot. Comput. Manuf.* **2014**, *30*, 189–200. [\[CrossRef\]](#)
8. Ashagrie, A.; Salau, A.O.; Weldcherkos, T. Modeling and control of a 3-DOF articulated robotic manipulator using self-tuning fuzzy sliding mode controller. *Cogent Eng.* **2021**, *8*, 1950105. [\[CrossRef\]](#)
9. Obando, C.; Chávez, D.; Leica, P.; Camacho, O. Sliding Mode Controller Based on a Hybrid Surface for Tracking Improvement of Non-Linear Processes. *IFAC-Pap.* **2020**, *53*, 11747–11752. [\[CrossRef\]](#)
10. Zhao, R.; Yang, J.; Li, X.; Mo, H. Adaptive Variable Universe Fuzzy Sliding-Mode Control for Robot Manipulators with Model Uncertainty. *IEEE J. Radio Freq. Identif.* **2024**, *8*, 658–664. [\[CrossRef\]](#)
11. Li, Z.; Zhai, J. Event-Triggered Based Sliding Mode Asymptotic Tracking Control of Robotic Manipulators. *IEEE Trans. Circuits Syst. II: Express Briefs* **2023**, *71*, 1266–1270. [\[CrossRef\]](#)
12. Ma, Z.; Sun, G. Dual terminal sliding mode control design for rigid robotic manipulator. *J. Frankl. Inst.* **2018**, *355*, 9127–9148. [\[CrossRef\]](#)
13. Azeez, M.I.; Abdelhaleem, A.M.M.; Elnaggar, S.; Moustafa, K.A.F.; Atia, K.R. Optimized sliding mode controller for trajectory tracking of flexible joints three-link manipulator with noise in input and output. *Sci. Rep.* **2023**, *13*, 12518. [\[CrossRef\]](#) [\[PubMed\]](#)
14. Naik, P.R.; Samantaray, J.; Roy, B.K.; Pattanayak, S.K. 2-DOF robot manipulator control using fuzzy PD control with SimMechanics and sliding mode control: A comparative study. In Proceedings of the 2015 International Conference on Energy, Power and Environment: Towards Sustainable Growth (ICEPE), Shillong, India, 12–13 June 2015; pp. 1–6. [\[CrossRef\]](#)
15. Vijay, M.; Jena, D. Optimal GA based SMC with adaptive PID sliding surface for robot manipulator. In Proceedings of the 2014 9th International Conference on Industrial and Information Systems (ICIIS), Gwalior, India, 15–17 December 2014; pp. 1–6. [\[CrossRef\]](#)
16. Azeez, M.I.; Elnaggar, S.; Abdelhaleem, A.M.M.; Moustafa, K.A.F.; Atia, K.R. Enhancing robustness and noise rejection in flexible joint manipulators: An optimized sliding mode controller with enhanced gray wolf optimization for trajectory tracking. *J. Braz. Soc. Mech. Sci. Eng.* **2023**, *45*, 4–7. [\[CrossRef\]](#)
17. Roberti, F.; Soria, C.; Slawinski, E.; Mut, V.; Carelli, R. Open Software Structure for Controlling Industrial Robot Manipulators. In *Robot Manipulators Trends and Development*; INTECH Open Access Publisher: Rijeka, Croatia, 2010; pp. 497–520. [\[CrossRef\]](#)
18. Orozco-Soto, S. Fuzzy PD+G Type 2 Interval Fuzzy PD+G Control for Position Control of Robot Manipulators. *Technol. Mag.* **2015**, *2*, 899–909.
19. Lozano, R.; Valera, A.; Albertos, P.; Arimoto, S.; Nakayama, T. PD control of robot manipulators with joint flexibility, actuators dynamics and friction. *Automatica* **1999**, *35*, 1697–1700. [\[CrossRef\]](#)

**Disclaimer/Publisher's Note:** The statements, opinions and data contained in all publications are solely those of the individual author(s) and contributor(s) and not of MDPI and/or the editor(s). MDPI and/or the editor(s) disclaim responsibility for any injury to people or property resulting from any ideas, methods, instructions or products referred to in the content.